Available online at www.sciencedirect.com

SCIENCE DIRECT

European Journal of Pharmacology 499 (2004) 35–44

www.elsevier.com/locate/ejphar

The respective *N*-hydroxypyrazole analogues of the classical glutamate receptor ligands ibotenic acid and (*RS*)-2-amino-2-(3-hydroxy-5-methyl-4-isoxazolyl)acetic acid

Rasmus P. Clausen[a,*], Kasper B. Hansen[a,b], Patrizia Calí[a], Birgitte Nielsen[a], Jeremy R. Greenwood[a], Mikael Begtrup[a], Jan Egebjerg[b], Hans Bräuner-Osborne[a]

[a]*Department of Medicinal Chemistry, Danish University of Pharmaceutical Sciences, 2 Universitetsparken, DK-2100 Copenhagen, Denmark*
[b]*Department of Molecular Biology, H. Lundbeck A/S, Ottiliavej 9, DK-2500 Valby, Denmark*

Received 25 March 2004; received in revised form 1 July 2004; accepted 6 July 2004
Available online 25 August 2004

Abstract

We have determined the pharmacological activity of *N*-hydroxypyrazole analogues (**3a** and **4a**) of the classical glutamate receptor ligands ibotenic acid and (*RS*)-2-amino-2-(3-hydroxy-5-methyl-4-isoxazolyl)acetic acid (AMAA), as well as substituted derivatives of these two compounds. The pharmacological profile of **3a** is closer to that of thioibotenic acid rather than ibotenic acid, while **4a** is a selective *N*-methyl-D-aspartic acid (NMDA) receptor agonist. Ring substitution of **3a** and **4a** leads to NMDA receptor antagonists. Whereas efficacy of **3a** derivatives at $mglu_2$ receptor decreases from agonism via partial agonism to antagonism with increasing substituent size, substitution abolishes affinity for $mglu_1$ and $mglu_4$ receptors. Ligand- and receptor-based modelling approaches assist in explaining these pharmacological trends among the metabotropic receptors and suggest a mechanism of partial agonism at $mglu_2$ receptor similar to that proposed for the GluR2 glutamate receptor.

Keywords: Ibotenic acid; Glutamate receptor; Metabotropic glutamate receptor; Docking; *N*-Hydroxypyrazole; Partial agonism

1. Introduction

Two distinct receptor classes are activated by the major excitatory neurotransmitter of the central nervous system (*S*)-glutamic acid: ionotropic receptors which are ligand-gated ion channels; and the G protein-coupled metabotropic receptors. So far, 16 ionotropic glutamate receptor subunits and 8 metabotropic glutamate receptor subtypes have been identified in humans (Bräuner-Osborne et al., 2000; Conn and Pin, 1997; Dingledine et al., 1999), forming the functional receptors involved in many physiological processes such as learning, memory, vision, control of movement and pain sensitivity (Holscher et al., 1999; Riedel et al., 2003). Ionotropic glutamate receptors are further subdivided into three groups, named after the selective agonists *N*-methyl-D-aspartic acid (NMDA), (*RS*)-2-amino-3-(hydroxy-5-methyl-4-isoxazolyl)propionic acid (AMPA) and kainate receptors. AMPA receptors are assemblies of subunits GluR1–4, while kainate receptors assemble from GluR5–7 and KA1–2, and NMDA receptors from NR1, NR2A–D and NR3A–B (Bräuner-Osborne et al., 2000; Dingledine et al., 1999).

Likewise, metabotropic glutamate receptors are divided into three groups. Group I consists of $mglu_1$ and $mglu_5$, which are coupled to the hydrolysis of phosphatidylinositol. The $mglu_2$ and $mglu_3$ receptors constitute group II and are coupled to inhibition of cyclic AMP formation. Group III comprises $mglu_4$, $mglu_6$, $mglu_7$ and $mglu_8$, which are also negatively linked to adenylyl cyclase activity (Conn and Pin, 1997).

* Corresponding author. Tel.: +45 35 30 61 14; fax: +45 35 30 60 40.
E-mail address: rac@dfuni.dk (R.P. Clausen).

0014-2999/$ - see front matter © 2004 Elsevier B.V. All rights reserved.
doi:10.1016/j.ejphar.2004.07.049

Dysfunction of the glutamatergic pathways have been implicated in a variety of neuropathologies, including epilepsy, stroke, cognitive disorders, and neurodegenerative diseases (Bräuner-Osborne et al., 2000; Dingledine et al., 1999; Holscher et al., 1999). The various components of the entire receptor system are potentially open to exploitation as therapeutic targets, and ligands that selectively affects these components continue to provide insight into the central functions of glutamate, as well as providing drug candidates (Bräuner-Osborne et al., 2000).

Many of the known selective ligands for the glutamate receptors have been derived from natural ligands such as (*S*)-glutamic acid itself. Ibotenic acid (Fig. 1) is a neurotoxic natural product from *Amanita muscaria* with the ability to affect several components of the glutamatergic system (Krogsgaard-Larsen and Hansen, 1992). The acidic 3-hydroxyisoxazole moiety in ibotenic acid serves as a bioisosteric substitute for the distal carboxylic acid in (*S*)-glutamic acid, and extensive modification of ibotenic acid have led to a number of highly selective glutamate receptor ligands based on this bioisostere, such as AMPA and (*RS*)-2-amino-2-(3-hydroxy-5-methyl-4-isoxazolyl)acetic acid (AMAA) (Bräuner-Osborne et al., 2000). Ibotenic acid has also been a source of inspiration for other carboxylate bioisosteres, and a number of heterocycles have been developed along these lines, in some cases giving rise to ligands with new pharmacological profiles, such as thio-

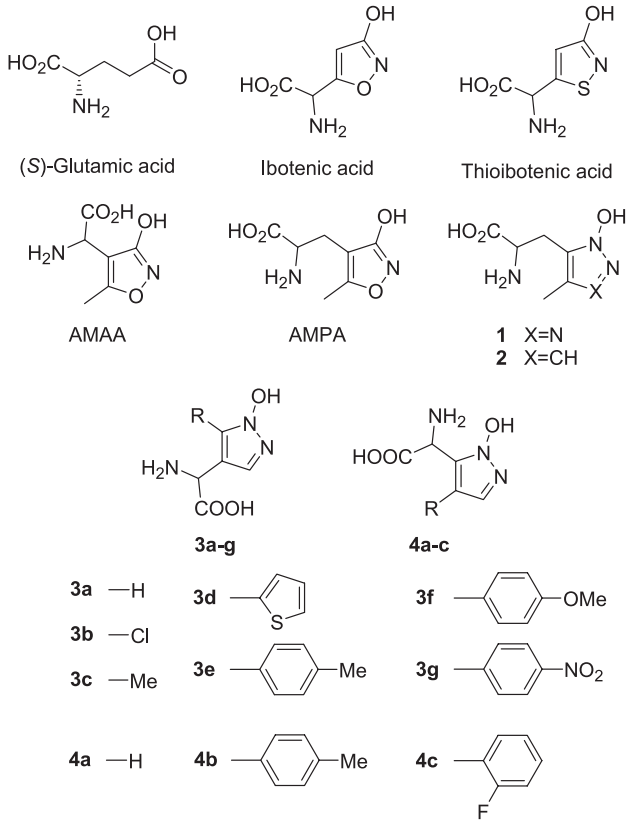

Fig. 1. Structures of glutamate receptor ligands including the substituted *N*-hydroxypyrazole analogues of ibotenic acid and AMAA, **3a–g** and **4a–c**.

ibotenic acid (Hermit et al., 2004). The 1-hydroxy-triazole and -pyrazole analogues of AMPA, **1** and **2** respectively, are recent examples of (*S*)-glutamic acid analogues bearing new carboxylate bioisosteres (Stensbøl et al., 2002).

Furthering this line of investigation, the synthesis of a number of 1-hydroxypyrazolyl glycine derivatives was recently reported by our department (Cali and Begtrup, 2002). These structures are 1-hydroxypyrazole analogues of ibotenic acid (**3a–g**) and AMAA (**4a–c**) and here we present the pharmacology of these ligands.

2. Materials and methods

2.1. Materials

1-Hydroxypyrazole glycine derivatives **3a–g** and **4a–c** were synthesised as previously described (Cali and Begtrup, 2002). (*S*)-2-Amino-4-phosphono-butyric acid (L-AP4), [^{3}H]L-AP4 (45.5 Ci mmol^{-1}), 2-amino-(3-hydroxy-5-isoxazolyl)acetic acid (ibotenic acid) and L-serine-*O*-phosphate (L-SOP), were purchased from Tocris Cookson (Bristol, UK). [^{3}H]AMPA (55.5 Ci mmol^{-1}), [^{3}H]kainic acid (55.5 Ci mmol^{-1}) and [^{3}H](*RS*)-(E)-2-amino-4-phosphonomethyl-3-heptenoic acid (CGP39653) were purchased from NEN (Boston, MA, USA). All other reagents were from Sigma-Aldrich (Munich, Germany).

2.2. Cell cultures

The Chinese hamster ovary (CHO) cell lines stably expressing rat mglu$_{1a}$, mglu$_2$ and mglu$_{4a}$ have previously been described (Aramori and Nakanishi, 1992; Tanabe et al., 1992, 1993).

Cells were cultured in Dulbecco's Modified Eagle Medium (DMEM) containing Glutamax-I and supplemented with penicillin (100 U/ml), streptomycin (100 mg/ml), and 10% dialysed fetal calf serum (all Invitrogen, Paisley, UK). In addition, media for metabotropic glutamate receptor subtypes 1a, 2 and 4a expressing cell lines contained 1% proline. Cells were maintained at 37 °C, 95% humidified air, 5% CO_2 in an incubator, and subcultured every 3–4 days.

2.3. Measurement of intracellular Ca^{2+} levels and cyclic AMP formation

Pharmacological activity at mglu$_{1a}$ was assessed by measurement of intracellular Ca^{2+} levels as previously described (Bjerrum et al., 2003). The day before pharmacological assays, 2×10^6 cells were split into one 96-well black-walled, clear-bottomed tissue culture plate with cell culture medium and incubated overnight. The following day, the measurement of intracellular calcium was performed as follows. The media was exchanged with Hanks balanced saline solution containing 1 mM $CaCl_2$, 1 mM

$MgCl_2$, 20 mM HEPES, 2.5 mM probenecid and 4 μM Fluo-4AM (pH 7.4). The cells were incubated for 1 h at 37 °C in a humidified 5% CO_2 incubator. Cells were then washed twice with the same buffer without Fluo-4AM and finally 100 μl of the buffer was left in the wells.

The cell plate was then transferred to a NovoStar (BMG Labtechnologies, Offenburg, Germany) and the basal fluorescence level was adjusted to ~10,000 fluorescence units (FU) using excitation/emission wavelengths of 485 and 520 nm, respectively. Fluorescence readings were measured for 45 s after addition of ligand and response was calculated as peak response minus basal level. Inactive compounds were also tested as antagonists. Twenty minutes after application of ligand, 20 μM (*S*)-glutamic acid was added to the well and fluorescence was measured as above.

Pharmacological activity at $mglu_2$ and $mglu_{4a}$ was assessed by measuring intracellular cAMP levels as previously described (Bräuner-Osborne and Krogsgaard-Larsen, 1998). Two days before the assay, 1 million cells were divided into the wells of a 96-well plate. On the day of the cyclic AMP assay, cells were preincubated for 20 min in phosphate buffer saline (PBS) with 1 mM 3-isobutyl-1-methylxanthine (IBMX) and then incubated for 10 min in a similar buffer including 10 μM forskolin and the ligand. The agonist activity was then determined as the inhibitory effect of the forskolin-induced cyclic AMP formation. Cyclic AMP levels were determined by use of a scintillation proximity assay according to the manufacturer's protocol (Amersham Biosciences, Uppsala, Sweden).

2.4. Binding assays at native ionotropic glutamate receptors

Rat brain membrane preparations used in the receptor binding experiments were prepared according to the method described by Ransom and Stec (1988). Affinities for native AMPA, kainate and NMDA receptors were determined using 5 nM [^{3}H]AMPA (Honore and Nielsen, 1985), 5 nM [^{3}H]kainic acid (Braitman and Coyle, 1987), and 2 nM [^{3}H]CGP39653 (Braitman and Coyle, 1987; Honore and Nielsen, 1985; Sills et al., 1991) with some modifications. On the day of experiments, frozen membranes were quickly thawed and homogenised in 40 volumes of ice-cold buffer (pH 7.4) (30 mM Tris–HCl containing 2.5 mM $CaCl_2$, 50 mM Tris–HCl, or 50 mM Tris–HCl containing 2.5 mM $CaCl_2$, for [^{3}H]AMPA, [^{3}H]kainate, or [^{3}H]CGP39653 binding, respectively), and centrifuged at 48.000×*g* for 10 min. This step was repeated four times. In [^{3}H]AMPA binding experiments, 100 mM potassium thiocyanate (KSCN) was added to the buffer during the final wash and during incubation. The final pellet was re-suspended in ice-cold buffer, corresponding to approx. 0.4−0.5 mg protein/ml. [^{3}H]AMPA, [^{3}H]kainate, and [^{3}H]CGP39653 binding were carried out in aliquots consisting of radioligand (25 μl), test solution (25 μl) and membrane suspension (200 μl), and incubated for 30, 60, and 60 min, respectively. Binding was terminated by filtration through GF/B filters using a 96-well Packard Filter-Mate Cell Harvester and washing with 3×250 μl buffer. After drying, 25 μl microscint 0 (Perkin-Elmer, Meriden, CT, USA) per well was added and the plate was counted on a Topcounter (Perkin-Elmer). Non-specific binding was determined using 1 mM (*S*)-glutamic acid.

2.5. Electrophysiology

For expression in *Xenopus* oocytes, rat NR1–1a, NR2A, NR2B, and NR2C were subcloned into pCI-neo containing a T7 site upstream from the 5′ untranslated region (UTR). Linearised plasmids were used to produce NR1–1a, NR2A, NR2B, and NR2C cRNAs with mMessage mMachine kits (Ambion, Huntingdon, UK). Oocytes were surgically removed from mature female *Xenopus laevis* anaesthetised in a 0.4% MS-222 (3-aminobenzoic acid ethyl ester) solution for 10–15 min. In order to remove the follicle layer, the oocytes were subsequently digested with 0.5 mg/ml collagenase (type IA) in OR-2 buffer (in mM: 82.5 NaCl, 2.0 KCl, 1.0 $MgCl_2$, and 5.0 HEPES; pH 7.5) at room temperature for 1.5–3 h. Healthy-looking stage V–VI oocytes were selected for injection the following day. Oocytes were co-injected with cRNA encoding NR1–1a and either of the NR2 subunits at a 1:3 ratio, respectively, and maintained in Barth's solution (in mM: 88 NaCl, 1.0 KCl, 2.4 $NaHCO_3$, 0.41 $CaCl_2$, 0.82 $MgSO_4$, 0.3 $Ca(NO_3)_2$, 15 HEPES; pH 7.5, 2% sodium pyruvate, 100 IU/ml penicillin, and 100 μg/ml streptomycin) at 18 °C. Recordings were performed 2–4 days after injection using whole-cell two-electrode voltage-clamp at −40 to −100 mV in bath solution containing (in mM) 115 NaCl, 2.5 KCl, 1.9 $BaCl_2$, and 10 HEPES (pH 7.5).

2.6. Data analysis

Pharmacological experiments were performed in duplicate or triplicate of at least three independent experiments. Single concentration tests were performed in triplicate with two independent experiments. Concentration–response and homologous displacement curves were analysed by non-linear regression using GraphPad Prism (GraphPad Software, San Diego, USA). K_i values were calculated from IC_{50} values by use of the Cheng and Prusoff (1973) equation. Numbers in parentheses [min, max] indicate ±S.E.M. according to a logarithmic distribution.

Electrophysiological data was acquired using Clampex 7.0 (Axon Instruments, Union City, CA, USA) and subsequently processed with GraphPad Prism. Agonist dose–response data for individual oocytes were fit to the equation

$$I = I_{\max}\frac{[\text{agonist}]^n}{EC_{50}^n + [\text{agonist}]^n}$$

where I is the current, I_{max} is the maximum current in response to the action of the agonist, and n denotes the Hill

coefficient. Relative maximal currents (relative I_{max}) were calculated as $I_{max,agonist}/I_{max,(S)\text{-glutamic acid}}$ where $I_{max,agonist}$ and $I_{max,(S)\text{-glutamic acid}}$ is the fitted I_{max} according to the equation (see above). Antagonist dose–response data for individual oocytes were fit to the equation

$$I = I_{max} - I_{max}\frac{[\text{antagonist}]^n}{IC_{50}^n + [\text{antagonist}]^n}$$

where I is the current, I_{max} is the maximum current in response to the action of the agonist, and n denotes the Hill coefficient. K_i was calculated according to the Cheng and Prusoff (1973) equation. $K_i = IC_{50}/(1+([\text{agonist}]/EC_{50}))$ using 2 μM (*S*)-glutamic acid as agonist. The mean and S.E.M. was calculated assuming a logarithmic distribution of EC_{50} and IC_{50} values.

2.7. Docking

Protein preparation using Impact 2.5/optimised potentials for liquid simulations-all atom (OPLS-AA) and calculation of grids for docking using Glide 2.5 have been previously described for the experimental crystal structure of the extracellular binding domain of rat $mglu_1$ (1EWK.PDB), and for homology models of $mglu_2$ and $mglu_4$ built from this structure (Hermit et al., 2004). The native ligand, tri-ionised (*S*)-glutamic acid, was included in the refinement process. The ligands were submitted to Monte Carlo analysis in tri-ionised forms using the Merck molecular force field (MMFFs) (Halgren, 1999a,b) including the "Generalized Born/Solvent Accessible Surface Area" (GB-SA) treatment of aqueous solvation in Macromodel 8.1 (Schrödinger, Portland, USA). Two minima were found for **3a–g**: C5–C4–C–H dihedral approximately 0° ('eclipsed') and 180° ('anti'); however, MMFFs assign a lower energy to the 'eclipsed form' of all compounds except **3a** where the 'anti' form was marginally favoured. As previously performed with ibotenic acid and thioibotenic acid, all compounds were flexibly docked with Glide to the agonist binding sites of $mglu_1$, $mglu_2$ and $mglu_4$ receptors using the 'eclipsed' form as the input structure. Due to neglect of intramolecular non-bonded interactions during the flexible docking process, in some cases it was necessary to co-minimise the docked poses in the receptor to relieve ligand strain; the MMFFs force field including GB-SA treatment of aqueous solvation in Macromodel 8.1 was used for this purpose.

2.8. Ab initio potential energy surface

Since the zwitterions of α-amino acids are generally not minima in gas phase, conformational analysis of the bioactive forms requires solution-phase optimisation. The conformational energies of **3a** and **3b** in solution and the internal energies (defined as the gas phase energies at the solution phase geometries) were studied using Density Functional Theory (B3LYP; Becke, 1993) with the 6-311+G(d,p) basis set (Krishnan et al., 1980) and Tomasi's polarisable continuum model of aqueous solvation employing the integral equation formalism (IEFPCM; Cancès and Mennucci, 2001) in Gaussian '03 (Gaussian, Pittsburg, USA). Starting from optimisations and analytical force constant calculations of the same tri-ionised forms of **3a** and **3b** in which the C4–C5–C–H dihedral was constrained to 0°, this coordinate was driven through 360° in 30° steps, optimising in solution at each step. Ultrafine integral grids and tight self-consistent field (SCF) convergence were used throughout, but for numerical reasons, loose criteria were used for geometry convergence. The solution phase partial minima were subjected to single-point gas phase calculations at the same level of theory to give the corresponding internal energies.

3. Results

3.1. Ionotropic glutamate receptor pharmacology

Initially, the compounds were tested for binding affinity to the ionotropic glutamate receptor groups AMPA, kainate and NMDA in a crude synaptosomal preparation. As shown in Table 1, most compounds had weak affinity to the NMDA receptors. In general, the *N*-hydroxypyrazole AMAA analogues **4a–c** had a higher affinity than the ibotenic acid analogues **3a–e**. No affinity to AMPA or kainate receptors could be observed, except for compound **3b**, which displays some AMPA receptor affinity.

This prompted the functional characterisation at cloned NMDA receptor subtypes of compounds displaying NMDA receptor affinity, including the classical NMDA receptor agonists NMDA and AMAA, and the antagonist 2-amino-5-phosphono-pentanoic acid (AP-5) (Table 2). This enabled agonists (**3a** and **4a**) to be distinguished from antagonists (**3b–e**, **4b**,**c**) as shown in Fig. 2A and B. All of the tested agonists apart from (*S*)-glutamic acid proved to be partial agonists in this assay. NMDA induced a steady state current 70–80% relative to the current induced by (*S*)-glutamic acid ($I_{max,(S)\text{-glutamic acid}}$). However, AMAA generated a current only 17% of $I_{max,(S)\text{-glutamic acid}}$ at NR1/NR2A receptors, but a 3-fold higher current at NR1/NR2B. Less variation was seen among the *N*-hydroxypyrazole derivatives, generally generating I_{max} 40–50% relative to $I_{max,(S)\text{-glutamic acid}}$ (Fig. 2A). The relationships among the EC_{50} values largely resembled those of the IC_{50} values from the rat brain binding assay, and no pronounced subtype selectivity was observed, but the compounds were more potent relative to (*S*)-glutamic acid than indicated by the binding assay. Substituting the heterocycles converts the agonists to antagonists, and a drop in potency is observed. Unlike the agonists, some of the antagonists

Table 1
Receptor binding affinity to ionotropic glutamate receptors in rat cortical membranes and potencies at recombinant rat metabotropic glutamate receptors of glutamate receptor ligands

	IC_{50} (μM)		K_i (μM)	EC_{50} (μM)/K_i (μM)[a]		
	[^{3}H]AMPA	[^{3}H]Kainic Acid	[^{3}H]CGP39653	$mglu_1$	$mglu_2$	$mglu_4$
(*S*)-glu	0.34[b]	0.38[b]	0.20 [0.16, 0.26]	10[c]	4.4[c]	10[c]
NMDA	>100[d]	>100[d]	6.2 [5.3, 7.4]	>1000[e]	>1000[f]	>1000[g]
AMAA	>100[d]	>100[d]	4.5[d]	>1000[c]	>1000[c]	>1000[c]
Ibo	>100[h]	22[h]	5.3[h]	43[h]	110[h]	>1000[h]
Thioibo	>100[h]	>100[h]	13[h]	12[h]	52[h]	2.6[h]
3a	>100	>100	39 [37, 41]	85 [64, 109]	230 [180, 280]	26 [10, 48]
3b	47 [44, 50]	>100	64 [61, 67]	>1000	51 [36, 68][i]	>1000
3c	>100	>100	56 [53, 60]	>1000	100 [57, 156]	>1000
3d	>100	>100	56 [48, 66]	>1000	**210 [150, 280]**	>1000
3e	>100	>100	>100	>1000	**140 [120, 150]**	>300
3f	>100	>100	>100	>1000	**180 [140, 230]**	>1000
3g	>100	>100	>100	>1000	**300 [230, 380]**	>1000
4a	>100	>100	10 [9, 11]	>1000	>1000	>1000
4b	>100	>100	34 [31, 38]	>1000	>1000	>1000
4c	>100	>100	30 [29, 31]	>1000	>1000	>1000

Functional data were obtained from CHO cell lines stably expressing the $mglu_{1,\ 2\ or\ 4}$ receptor subtype. Results on $mglu_1$ receptors were obtained by measurement of intracellular Ca^{2+} levels and EC_{50} values for $mglu_{2\ and\ 4}$ were determined using the cAMP assay. Data are given as means±S.E.M. [min, max] of at least three independent experiments according to a logarithmic distribution.

[a] Antagonism in bold.
[b] Data from Johansen et al. (2002).
[c] Data from Bräuner-Osborne et al. (1996).
[d] Data from Madsen et al. (1990); IC_{50} of [^{3}H]CPP binding instead of K_i of [^{3}H]CGP39653 binding.
[e] Data from Aramori and Nakanishi (1992).
[f] Data from Tanabe et al. (1992).
[g] Data from Tanabe et al. (1993).
[h] Data from Hermit et al. (2004).
[i] Partial agonism: 67±11% of maximal response.

display low but significant subtype selectivity, generally with a preference for the NR1/NR2A receptors. Thus, **4b** is 5-fold more potent at NR1/NR2A receptors than NR1/NR2C receptors.

3.2. Metabotropic glutamate receptor pharmacology

The *N*-hydroxypyrazole analogues of AMAA **4a–c** had no effect on any of the metabotropic glutamate receptors

Table 2
Agonist and antagonist effects at cloned rat NMDA receptors combining NR1–1a with the subunits NR2A, NR2B and NR2C, respectively

Agonists

	NR1–1a/NR2A			NR1–1a/NR2B			NR1–1a/NR2C		
	EC_{50} (μM)	n_H	Relative I_{max}	EC_{50} (μM)	n_H	Relative I_{max}	EC_{50} (μM)	n_H	Relative I_{max}
(*S*)-glu	2.9 [2.5, 3.2]	1.1	1	1.8 [1.5, 2.1]	1.6	1	1.5 [1.3, 1.7]	1.2	1
NMDA	46 [41, 52]	1.5	0.80±0.02	31 [29, 33]	1.7	0.77±0.06	22 [21, 23]	1.5	0.68±0.01
AMAA	21 [18, 23]	1.7	0.17±0.01	29 [26, 31]	1.5	0.51±0.01	41 [37, 46]	1.5	0.32±0.02
3a	140 [130, 150]	1.7	0.39±0.04	140 [130, 150]	1.8	0.38±0.01	127 [122, 132]	1.4	0.45±0.03
4a	82 [75, 90]	1.3	0.45±0.03	48 [47, 49]	1.6	0.58±0.02	54 [50, 57]	1.4	0.52±0.01

Antagonists

	NR1–1a/NR2A		NR1–1a/NR2B		NR1–1a/NR2C	
	IC_{50} (μM)	K_i (μM)	IC_{50} (μM)	K_I (μM)	IC_{50} (μM)	K_i (μM)
AP5	1.3 [1.2, 1.4]	0.74	3.9 [3.2, 4.8]	1.9	3.6 [3.4, 3.9]	1.5
3b	370 [320, 430]	220	>1500	>700	650 [580, 720]	280
3c	310 [260, 370]	180	320 [270, 370]	150	620 [560, 690]	270
3d	230 [210, 260]	140	520 [510, 530]	250	1300 [1270, 1320]	550
4b	210 [180, 230]	120	280 [260, 300]	130	1370 [1300, 1440]	580
4c	210 [180, 250]	130	260 [250, 270]	120	500 [470, 550]	220

Measurements performed on cloned receptors expressed in *Xenopus* oocytes using a whole-cell two-electrode voltage-clamp. Data are given as means±S.E.M. of at least three independent experiments.

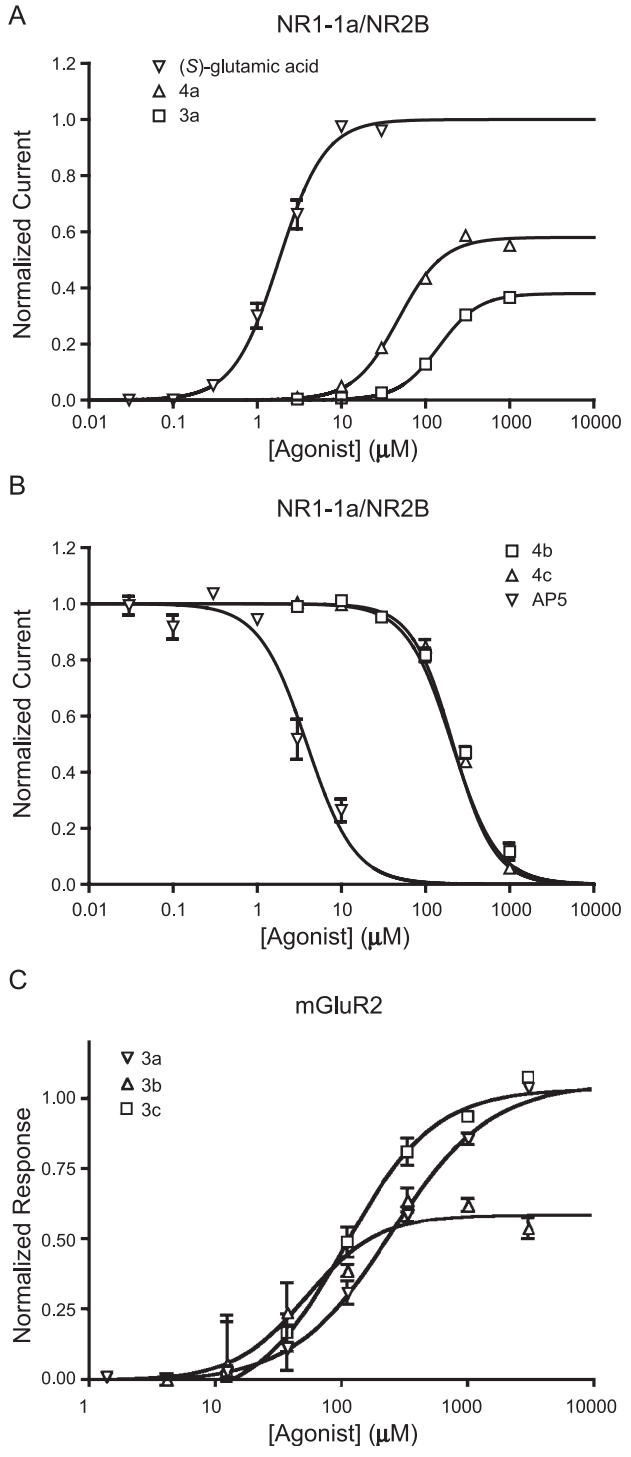

Fig. 2. Concentration–response curves of agonist-induced currents relative to maximal (*S*)-glutamic acid induced currents (A) and concentration-dependent inhibition curves of (*S*)-glutamic acid induced currents (B) from NR1–1a/NR2B expressing *Xenopus* oocytes. (C) Concentration–response curves of agonist-induced inhibition of cyclic AMP production relative to maximal (*S*)-glutamic acid response from CHO cell line stably expressing the $mglu_2$ receptor subtype.

tested (Table 1), whereas the ibotenic acid analogue **3a** was active at all three groups of metabotropic receptors, as represented by $mglu_1$, $mglu_2$ and $mglu_4$. At $mglu_1$ and $mglu_2$, **3a** was 2-fold less potent than ibotenic acid and 4-fold less potent than thioibotenic acid. Unlike ibotenic acid, activity at $mglu_4$ was observed, but potency was 10-fold lower than that of thioibotenic acid. Activity at $mglu_1$ and $mglu_4$ was abolished upon substitution at the 5-position of the heterocyclic ring, but the efficacy at $mglu_2$ migrated from agonism to antagonism via partial agonism depending on the size of the substituent. Thus, the methyl derivative **3c** is a full agonist, whereas the more protrusive chloro-substituted derivative **3b** is a partial agonist (Fig. 2C). Substitution with large aryl groups (**3d–g**) leads to antagonists, accompanied by a drop in potency. Interestingly, chlorination of the 5-position (**3b**) is accompanied by a gain in potency.

3.3. In silico

The internal energy (gas phase energy at solution phase geometry) and the aqueous phase energy of the trionised (*S*)-forms of **3a** and **3b** present at physiological pH and presumed active were investigated as a function of the dihedral angle between the α-amino acid and the ring. Given the strong polarisability and intra- and intermolecular electrostatic interactions of these ligands, and the exotic heterocyclic ring structures, calculations based on high-level quantum mechanics were employed, in conjunction with a continuum solvation model. The potential energy surfaces are summarised in Fig. 3. The global minima in solution have C5–C4–C–H dihedral angles of ca. 0° and 180° for both ligands, but their energies deviate when moving to other conformations. As expected, the rotational barrier is greater for **3b** due to the intramolecular sterics of the chloro substituent making this compound more conformationally restricted (Fig. 3B). The internal energy follows a similar trend to the solution phase energetics though with sharper gradients, and for both ligands, dihedral angles between 100° and 140° and in particular around 240° and 320° are unfavourable.

Compounds with activity at $mglu_2$ were docked into binding domain homology models of the agonised and antagonised state of this receptor (built from the open and closed forms of $mglu_1$) presuming the (*S*)-enantiomer to be the active species. The agonists **3a–c** docked into the agonised model of $mglu_2$ with favourable energy scores (Fig. 4A), whereas the bulkier aromatic groups in **3d–g** cannot be accommodated within the ligand binding site. On the other hand, poses with favourable energy scores resulted from docking **3d–g** in the antagonised model. However, due to neglect of intramolecular non-bonded interactions and the torsional parameters of the OPLS force field used in this version of Glide, the planes of the two aromatic rings were unreasonably eclipsed in the highest scoring poses, an unlikely situation due to vdw-repulsion by the ortho-hydrogens on the aromatic ring. The ligands and amino acid side chains within a radius of 16 Å were therefore subsequently

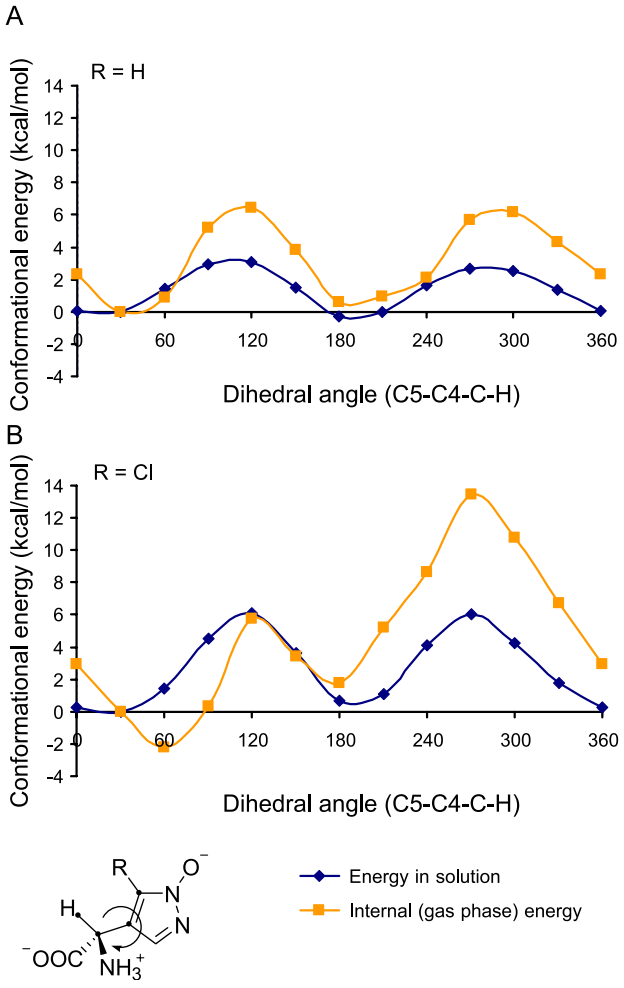

Fig. 3. Conformational energy (kcal/mol) of tri-ionised form as function of C5–C4–C–H dihedral angle in water (IEFPCM model) at B3LYP/6-311+G(d,p). Solution phase energy (blue) and gas phase internal energy (yellow) was calculated for (A) amino-(1-hydroxy-pyrazol-4-yl)-acetic acid (**3a**) and (B) amino-(5-chloro-1-hydroxy-pyrazol-4-yl)-acetic acid (**3b**).

minimised while constraining the backbone. This resulted in credible conformations with the aromatic rings out of plane shown in Fig. 4B. The methyl and chloro substituents in **3c** (green) and **3b** (not shown but overlaps **3c**), respectively, seems to be filling a lipophilic pocket lined by the methylene group of Gly296, the aromatic ring of Tyr216 and the methylenes of Arg271. These favourable contacts can explain their increased activity compared to the parent compound **3a** which have two plausible poses slightly twisted (~30°) from the anti and eclipsed (shown in Fig. 4B) conformations. Thioibotenic acid also points its sulphur ring towards this lipophilic cavity. The extent to which the chloro substituent of **3b** protrudes from the ring is greater than in **3a** and **3c**, suggesting that it would fit better into a slightly more opened form of the binding domain, which would account for the observed partial agonism by a mechanism similar to that postulated for the GluR2 receptor (Hogner et al., 2002). However, it cannot be excluded that partial agonism arises from opposite efficacies of the two enantiomers in the racemic mixture. Otherwise, the ligand–receptor interactions of the agonists to the depicted residues (Fig. 4) are similar to those of (*S*)-glutamic acid, as seen in previous studies with (*S*)-glutamic acid and (1*S*,2*S*,5*R*,6*S*)-2-aminobicyclo[3.1.0]-hexane-2,6-dicarboxylate (LY354740) at $mglu_2$ (Malherbe et al., 2001). The antagonists **3d**, **3f** and **3g** docked in the same C5–C4–C–H low-energy 'eclipsed' conformation, with the ionised groups interacting with residues in the lower ligand binding domain (LB1) (**3f** shown in pink). However, **3e** (grey) twists out the eclipsed conformation, possibly making a π-cation interaction with Lys377. Otherwise, the substituents simply point into the aqueous surroundings without beneficial interactions with the receptor, accounting for the low variance in potency.

In order to examine the loss of activity of **3b** and **3c** at $mglu_1$ and $mglu_4$ despite $mglu_2$ activity, **3a** was docked in these receptors. When docking **3a** in the agonised state of

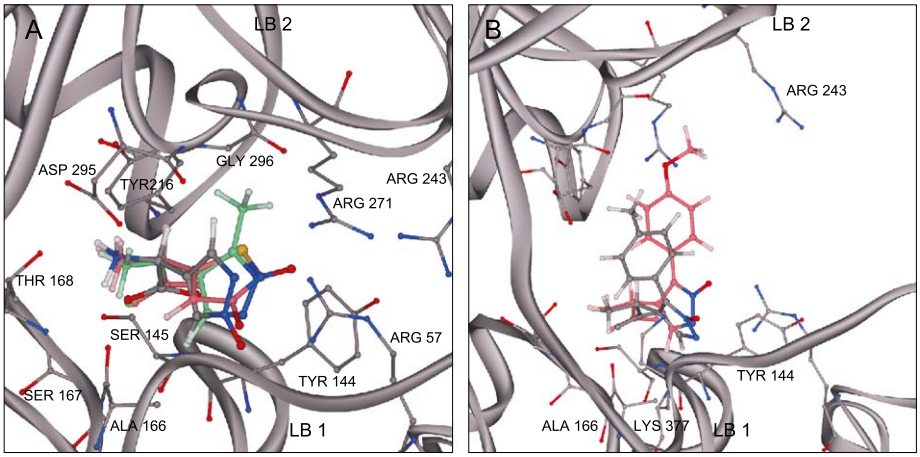

Fig. 4. (A) The agonists thioibotenic acid (pink), **3a** (grey) and **3c** (green), docked to a homology model of the closed ligand binding (LB) domain of $mglu_2$. The methyl group in **3c** fills a lipophilic cavity. (B) Antagonists **3e** (grey) and **3f** (pink), docked to a homology model of the open ligand binding domain of $mglu_2$.

$mglu_1$ the resulting poses spanned several conformations of the agonist. All but two of these conformations could be discarded due to large internal energy penalties, leaving the nearly 'eclipsed' (1°) and 'anti' (176°) conformations close to the two minima in solution (Fig. 3) as only possible conformations, docking with equal energy score. Thus, both conformations in principle could contribute to the agonist activity of **3a** in $mglu_1$. In Fig. 5A, the 'eclipsed' conformation of **3a** is shown together with (*S*)-glutamic acid, and moving the *N*-oxygen to the neighbouring nitrogen gives the 'anti' conformation pose. The same conformations are obtained when docking to the antagonised state of the receptor where the ligand interacts only with LB1. Introducing substituents in the 5-position would conflict with Gly319 in the upper ligand binding domain (LB2). Docking **3b** to $mglu_1$ gave only poses which could be discarded by a large internal energy penalty according to the ab initio analysis, for example a dihedral angle of 300° when accommodating the chloro substituent into the same lipophilic cavity as in $mglu_2$, spanned by Gly319, Tyr236 and Glu292 (corresponding to Gly296, Tyr216 and Arg271, respectively, in $mglu_2$). Docking **3a** in $mglu_4$ results in two conformations close to the internal energy minima, and one is shown in Fig. 5B with a C5–C4–C–H dihedral angle of 53°. Again, the other conformation (233°) can be obtained by moving the *N*-oxygen to the neighbouring nitrogen in the heterocycle. This twist corresponds to what we have previously proposed for thioibotenic acid, which is forbidden for ibotenic acid due to the high internal energy of this conformation which thus renders ibotenic acid inactive at $mglu_4$. The twist enables a favourable interaction of **3a** and thioibotenic acid with Lys405, which have previously been proven to be crucial for the binding of L-AP4 (Rosemond et al., 2002). As in $mglu_1$ the 5-substituted ligands cannot be accommodated in $mglu_4$ due to steric conflicts, this time with Asp312. Furthermore, the side chain of Ser313 in $mglu_4$ (corresponding to Gly296 in $mglu_2$) fill up the aforementioned cavity in $mglu_2$. In the antagonised state of $mglu_4$ **3a** docks only in a conformation close to anti (194°, shown in red, Fig. 5B). This conformation leaves no room for substituents at the 5-position but also lacks direct interaction with Lys405.

4. Discussion

Our previous report of a striking difference in the pharmacological profile of ibotenic acid and thioibotenic acid (Hermit et al., 2004) prompted the investigation of the biological activity of the structurally related 1-hydroxypyrazole analogues **3a** and **4a** at the glutamate receptors. Compound **3a** proved to have a pharmacological profile very similar to thioibotenic acid although in general the compound is less potent. Compound **4a** was found to be active only at NMDA receptors, as to be expected considering the close structural relationship to the classical NMDA receptor ligand AMAA. With access to substituted analogues of **3a** and **4a** we could probe how substitution affects the pharmacology of these two ligands. It turned out that substitution of the 5-position of the heterocycle of **3a** converted the $mglu_2$ agonism to antagonism via partial agonism depending on the size of the substituent. It is noteworthy that a similar trend could not be observed in $mglu_1$ and $mglu_4$; affinity to these receptors is simply lost upon substitution. The docking results suggests that partial agonism at $mglu_2$ is related to the degree of domain closure stabilised by the ligand as seen for the GluR2 receptor (Hogner et al., 2002). This is also suggested in a recent mutation study of the $mglu_8$ receptor, where the antagonism of (*S*)-2-amino-2-methyl-4-phosphonobutanoic acid (MAP4) is converted to partial agonist and

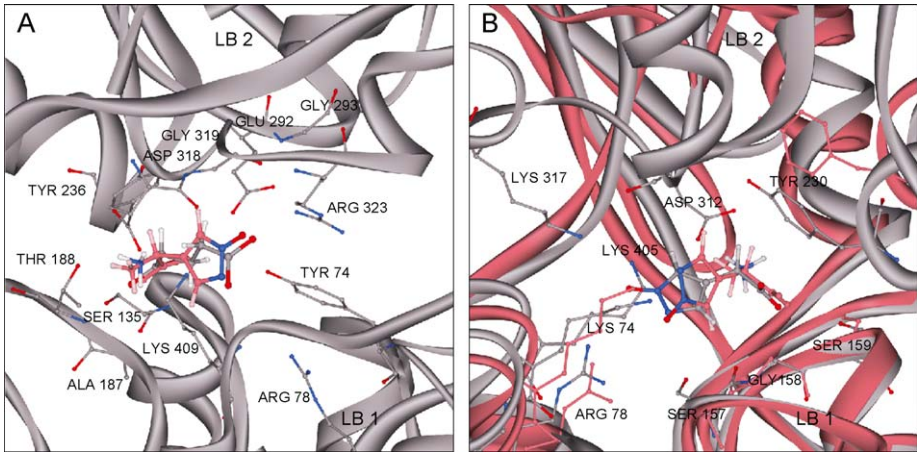

Fig. 5. (A) The agonists (*S*)-glutamic acid (grey) and (*S*)-**3a** (pink) docked to the closed ligand binding domain (LB) in the crystal structure of $mglu_1$. The same conformation of **3a** is obtained when docked to the open LB (not shown). (B) The conformations of **3a** obtained when docked in a closed/agonised (grey) and an open antagonist (pink) homology model of $mglu_4$.

agonist by exchanging Tyr227 (corresponding to Tyr216 and Tyr230 in $mglu_2$ and $mglu_4$, respectively) for Phe and Ala, respectively (Bessis et al., 2002).

Likewise the partial NMDA receptor agonism of **3a** and **4a** converted to antagonism upon substitution; however, in this receptor even a small substituent like the methyl group of **3c** abolishes agonism, unlike agonism at $mglu_2$, which tolerates this substituent. The striking differences in metabotropic glutamate receptor activity prompted docking studies in the quest for a structural explanation. These studies point to a lipophilic cavity in $mglu_2$ which is filled by the chloro and methyl substituent of **3b** and **3c**. This cavity is filled by a serine in $mglu_4$ and in $mglu_1$ it is only reached by a twist in the C5–C4–C–H dihedral angle leading to large penalty in internal energy. We have not been able to find an obvious explanation for why these ligands do not antagonise $mglu_1$ and $mglu_4$ but do agonise $mglu_2$. However, a distinguishing feature of the interaction of **3a** with $mglu_1$ and $mglu_4$ as opposed to $mglu_2$ is that of the heterocycle with the basic residues Arg323 and Lys317 in LB2 of $mglu_1$ and $mglu_4$, respectively, which will be lost upon binding to the open state of the ligand binding domain. In $mglu_2$ this residue is a leucine, and a strong polar interaction with Arg57 in LB1 (corresponding to Tyr74 in $mglu_1$ and Lys74 in $mglu_4$) that is crucial according to mutation studies (Malherbe et al., 2001) possibly compensate for the lack of interaction with basic residues in LB2. Although mutations of Arg323 in $mglu_1$ and Lys317 in $mglu_4$ to alanine does not alone affect the binding of (*S*)-glutamic acid and L-AP4, the double mutation of Lys317 and Lys74 in $mglu_4$ abolishes affinity to L-AP4 (Rosemond et al., 2002; Sato et al., 2003). This find supports the hypothesis that the loss of ligand hydrogen bonding to Arg323 in $mglu_1$ or Lys317 in $mglu_4$, together with the lack of other interactions to LB2 upon domain opening, could lead to the dramatic loss of affinity when substituents are introduced, whereas in $mglu_2$ affinity is sustained by Arg57.

Our results prove that the *N*-hydroxypyrazole can function as a versatile carboxylic acid bioisostere even though formally speaking there is no canonical form in which the negative charge resides solely on the unsubstituted ring nitrogen as it can in the case of isoxazole 3-oxyanion. Therefore, *N*-hydroxypyrazole analogues deserve a place in the medicinal chemist's toolkit, with the advantage over isoxazolols of an extra substitutable position. In addition, **3a** and **4a** provide interesting lead structures for the further design of glutamate receptor ligands and we are currently extending the synthetic series of these structures to refine their selectivity and potency. Our docking studies suggest that partial agonism at $mglu_2$ is related to the degree of domain closure stabilised by the ligand, similar to what has been shown for GluR2 (Hogner et al., 2002).

Acknowledgments

This work was supported by the Danish Medical Research Council and the Lundbeck Foundation. The CHO expressing cell lines were kind gifts from professor Shigetada Nakanishi, Kyoto University. Computer time was kindly provided by the Danish Center for Scientific Computing and the Australian Centre for Advanced Computing and Communications.

References

Aramori, I., Nakanishi, S., 1992. Signal transduction and pharmacological characteristics of a metabotropic glutamate receptor, mgluR1, in transfected CHO cells. Neuron 8, 757–765.

Becke, A.D., 1993. Density-functional thermochemistry: III. The role of exact exchange. J. Chem. Phys. 98, 5648–5652.

Bessis, A.S., Rondard, P., Gaven, F., Brabet, I., Triballeau, N., Prezeau, L., Acher, F., Pin, J.P., 2002. Closure of the Venus flytrap module of mGlu8 receptor and the activation process: insights from mutations converting antagonists into agonists. PNAS 97, 11097–11102.

Bjerrum, E.J., Kristensen, A.S., Pickering, D.S., Greenwood, J.R., Nielsen, B., Liljefors, T., Schousboe, A., Bräuner-Osborne, H., Madsen, U., 2003. Design, synthesis, and pharmacology of a highly subtype-selective GluR1/2 agonist, (*R*S)-2-amino-3-(4-chloro-3-hydroxy-5-isoxazolyl)propionic acid (Cl-HIBO). J. Med. Chem. 46, 2246–2249.

Braitman, D.J., Coyle, J.T., 1987. Inhibition of [^{3}H]kainic acid receptor binding by divalent cations correlates with ion affinity for the calcium channel. Neuropharmacology 26, 1247–1251.

Bräuner-Osborne, H., Krogsgaard-Larsen, P., 1998. Pharmacology of (*S*)-homoquisqualic acid and (*S*)-2-amino-5-phosphonopentanoic acid [(*S*)-AP5] at cloned metabotropic glutamate receptors. Br. J. Pharmacol. 123, 269–274.

Bräuner-Osborne, H., Sløk, F.A., Skjærbæk, N., Ebert, B., Sekiyama, N., Nakanishi, S., Krogsgaard-Larsen, P., 1996. A new highly selective metabotropic excitatory amino acid agonist: 2-amino-4-(3-hydroxy-5-methylisoxazol-4-yl)butyric acid. J. Med. Chem. 39, 3188–3194.

Bräuner-Osborne, H., Egebjerg, J., Nielsen, E.Ø., Madsen, U., Krogsgaard-Larsen, P., 2000. Ligands for glutamate receptors: design and therapeutic prospects. J. Med. Chem. 43, 2609–2645.

Cali, P., Begtrup, M., 2002. Synthesis of 1-hydroxypyrazole glycine derivatives. Tetrahedron 58, 1595–1605.

Cancès, E., Mennucci, B., 2001. Comment on "Reaction field treatment of charge penetration". J. Chem. Phys. 114, 4744–4745.

Cheng, Y., Prusoff, W.H., 1973. Relationship between the inhibition constant (K1) and the concentration of inhibitor which causes 50 per cent inhibition (I50) of an enzymatic reaction. Biochem. Pharmacol. 22, 3099–3108.

Conn, P.J., Pin, J.P., 1997. Pharmacology and functions of metabotropic glutamate receptors. Annu. Rev. Pharmacol. Toxicol. 37, 205–237.

Dingledine, R., Borges, K., Bowie, D., Traynelis, S.F., 1999. The glutamate receptor ion channels. Pharmacol. Rev. 51, 7–61.

Halgren, T.A., 1999a. MMFF: VI. MMFF94s option for energy minimization studies. J. Comp. Chem. 20, 720–729.

Halgren, T.A., 1999b. MMFF: VII. Characterization of MMFF94, MMFF94s, and other widely available force fields for conformational energies and for intermolecular-interaction energies and geometries. J. Comp. Chem. 20, 730–748.

Hermit, M.B., Greenwood, J.R., Nielsen, B., Bunch, L., Jørgensen, C.G., Vestergaard, H.T., Stensbøl, T.B., Sanchez, C., Krogsgaard-Larsen, P., Madsen, U., Bräuner-Osborne, H., 2004. Ibotenic acid and thioibotenic acid: a remarkable difference in activity at group III metabotropic glutamate receptors. Eur. J. Pharmacol. 486, 241–250.

Hogner, A., Kastrup, J., Jin, R., Liljefors, T., Mayer, M., Egebjerg, J., Larsen, I., Gouaux, E., 2002. Structural basis for AMPA receptor activation and ligand selectivity: crystal structures of five agonist complexes with the GluR2 ligand-binding core. J. Mol. Biol. 322, 93.

Holscher, C., Gigg, J., O'Mara, S.M., 1999. Metabotropic glutamate receptor activation and blockade: their role in long-term potentiation, learning and neurotoxicity. Neurosci. Biobehav. Rev. 23, 399–410.

Honore, T., Nielsen, M., 1985. Complex structure of quisqualate-sensitive glutamate receptors in rat cortex. Neurosci. Lett. 54, 27–32.

Johansen, T.N., Janin, Y.L., Nielsen, B., Frydenvang, K., Bräuner-Osborne, H., Stensbøl, T.B., Vogensen, S.B., Madsen, U., Krogsgaard-Larsen, P., 2002. 2-Amino-3-(3-hydroxy-1,2,5-thiadiazol-4-yl)propionic acid: resolution, absolute stereochemistry and enantiopharmacology at glutamate receptors. Bioorg. Med. Chem. 10, 2259–2266.

Krishnan, R., Binkley, J.S., Seeger, R., Pople, J.A., 1980. Self-consistent molecular-orbital methods: XX. Basis set for correlated wave-functions. J. Chem. Phys. 72, 650–654.

Krogsgaard-Larsen, P., Hansen, J.J., 1992. Naturally-occurring excitatory amino acids as neurotoxins and leads in drug design. Toxicol. Lett., 64–65. (Spec. No. 409–416).

Madsen, U., Ferkany, J.W., Jones, B.E., Ebert, B., Johansen, T.N., Holm, T., Krogsgaard-Larsen, P., 1990. NMDA receptor agonists derived from ibotenic acid. Preparation, neuroexcitation and neurotoxicity. Eur. J. Pharmacol., Mol. Pharmacol. 189, 381–391.

Malherbe, P., Knoflach, F., Broger, C., Ohresser, S., Kratzeisen, C., Adam, G., Stadler, H., Kemp, J.A., Mutel, V., 2001. Identification of essential residues involved in the glutamate binding pocket of the group II metabotropic glutamate receptor. Mol. Pharmacol. 60, 944–954.

Ransom, R.W., Stec, N.L., 1988. Cooperative modulation of [^{3}H]MK-801 binding to the *N*-methyl-D-aspartate receptor-ion channel complex by L-glutamate, glycine, and polyamines. J. Neurochem. 51, 830–836.

Riedel, G., Platt, B., Micheau, J., 2003. Glutamate receptor function in learning and memory. Behav. Brain Res. 140, 1–47.

Rosemond, E., Peltekova, V., Naples, M., Thøgersen, H., Hampson, D.R., 2002. Molecular determinants of high affinity binding to group III metabotropic glutamate receptors. J. Biol. Chem. 277, 7333–7340.

Sato, T., Shimada, Y., Nagasawa, N., Nakanishi, S., Jingami, H., 2003. Amino acid mutagenesis of the ligand binding site and the dimer interface of the metabotropic glutamate receptor 1. Identification of crucial residues for setting the activated state. J. Biol. Chem. 278, 4314–4321.

Sills, M.A., Fagg, G., Pozza, M., Angst, C., Brundish, D.E., Hurt, S.D., Wilusz, E.J., Williams, M., 1991. [^{3}H]CGP 39653: a new *N*-methyl-D-aspartate antagonist radioligand with low nanomolar affinity in rat brain. Eur. J. Pharmacol. 192, 19–24.

Stensbøl, T.B., Uhlmann, P., Morel, S., Eriksen, B.L., Felding, J., Kromann, H., Hermit, M.B., Greenwood, J.R., Bräuner-Osborne, H., Madsen, U., Junager, F., Krogsgaard-Larsen, P., Begtrup, M., Vedsø, P., 2002. Novel 1-hydroxyazole bioisosteres of glutamic acid. Synthesis, protolytic properties, and pharmacology. J. Med. Chem. 45, 19–31.

Tanabe, Y., Masu, M., Ishii, T., Shigemoto, R., Nakanishi, S., 1992. A family of metabotropic glutamate receptors. Neuron 8, 169–179.

Tanabe, Y., Nomura, A., Masu, M., Shigemoto, R., Mizuno, N., Nakanishi, S., 1993. Signal transduction, pharmacological properties, and expression patterns of two rat metabotropic glutamate receptors, mgluR3 and mgluR4. J. Neurosci. 13, 1372–1378.